DOI: 10.13009/EUCASS2019-723

DOI: ADD DOINUMBER HERE

Design of low-thrust control in the geostationary region for station keeping

Lincheng Li[⋆]*, Ioannis Gkolias*[⋆⋆]*, Camilla Colombo*[⋆⋆†]*, and Jingrui Zhang*[⋆]
[⋆]*School of Aerospace Engineering, Beijing Institute of Technology*
Zhongguancun South Str. 5, Haidian Dis., Beijing 100081, China
[⋆⋆] *Department of Aerospace Science and Technology, Politecnico di Milano*
Via La Masa 34, Milan 20156, Italy
lilincheng2012@163.com · ioannis.gkolias@polimi.it
camilla.colombo@polimi.it · zhangjingrui@bit.edu.cn
[†]Corresponding author

Abstract

This paper investigates low-thrust station-keeping strategies for geostationary satellites. On the contratry to traditional low-thrust control methods, which requires ground-station operations in a daily basis, the proposed method maximises the exploitation of natural dynamics and allows for the design of an efficient control within a predefined slot. The dynamical model, based on a spherical coordinate representation, is explored with analytical and numerical techniques to study the phase space. Minimum-time and minimum-fuel methods are implemented to design the maneuvers and the two-point boundary value problem is solved via an initial costate evaluation method.

1. Introduction

Geostationary (GEO) satellites are playing an increasingly important role in the field of navigation, communication, early warning and remote sensing[1] . Geostationary satellites are typically controlled to maintain a predefined geostationary slot. Osculating and mean orbital dynamics of satellites in the geostationary region are studied through different representations[2,3] . Resonant phenomena[4] at geosynchronous altitude are continously researched and provide potential alternatives to orbital transfer design, station-keeping[5] and end-of-life disposal[6,7] .

Chemical propulsion (impulsive) and electric propulsion (low-thrust) systems are the two main alternatives to achieve the required station-keeping. Compared to impulsive station-keeping, the low-thrust strategies have the advantage of a high specific impulse, which results in significant cost savings. With the advance of all-electrical geostationary satellite platforms, the design of efficient low-thrust station-keeping strategies is key to further reduce mission costs.

Due to the natural perturbations, satellites systematically drift away from their desired slots. Existing low-thrust control strategies, including open-loop[8,9] , closed-loop[10,11] and optimized methods[12–14] , employ frequent manoeuvres to completely eliminate the effects of perturbations. A frequent low-thrust control law (once a day or more frequently) gives the advantage of accurate positioning, however it comes with two main drawbacks. The first is the operational cost, as ground-station operations are required in a daily basis, leading to an increased mission cost. Moreover, new challenges arise in terms of satellite collocation (multiple satellites share one slot), especially in the GEO region where operational slots are limited.

In this work, we focus on low-thrust geostationary station-keeping design and propose a control method, which combines low-thrust maneuvers with the exploitation of the natural dynamics, as an alternative to reduce mission costs and enhance the GEO orbital capacity. The models used in this work are based on a spherical coordinate representation, while analytical and numerical approaches are used to study the in-plane and out-of-plane motion. According to the dynamical characteristics of the perturbed motion in longitude and latitude phase space, the controlled bounded motion in longitude and latitude are designed separately, in analogy of what is already done for chemical propelled GEO satellites. In order to increase the low-thrust control period and decrease the ground-station operational cost, a suitable combination of coast and low-thrust arcs is proposed to guarantee a smooth operational behaviors within a given slot. Finally, Minimum-time and minimum-fuel models are formulated, and an analytical Jacobian and initial costate evaluation method are proposed to solve the two-point boundary value problem.

DOI: 10.13009/EUCASS2019-723

2. In-plane motion and east-west station-keeping

In this section the equations of the in-plane motion are derived based on the spherical coordinate representation. The long-term dynamics induced purely from the tesseral contribution are studied. According to the phase space study, minimum-time and minimum-fuel models are formulated to achieve the confined motion within a longitude slot, achieving an efficient east-west station-keeping (EWSK).

2.1 J_{22} long-term dynamics

Compared to the classical orbital elements and modified equinoctial orbital elements[15] , earth-fixed spherical coordinates[16] are easier to be observed and computed. Let us assume an Earth-fixed polar coordinate system (r, λ, ϕ), with origin at the center of the Earth. λ is the satellite longitude relative to the direction of the vernal equinox, ϕ is the satellite latitude, and r is its radial distance from the center of the Earth. Since we focus only in the planar motion in this section, the assumption of relatively small latitude $\phi \approx 0°$ is considered in the following.

The components of acceleration in the direction of the unit vectors in the two-dimension earth-fixed spherical coordinate system are expressed as[16]

$$\begin{aligned} (a_r)_{sph} &= \ddot{r} - r\left(\Omega + \dot{\lambda}\right)^2 \\ (a_\lambda)_{sph} &= r\ddot{\lambda} + 2\dot{r}\left(\Omega + \dot{\lambda}\right) \end{aligned} , \tag{1}$$

where Ω is the angular rotation rate of the Earth.

In order to understand the underlying characteristics of the in-plane motion in the GEO region, we only consider the perturbation to the two-body dynamics due to the Earth gravity field, which is conservative and can be described through a disturbing potential U. Due to the differences in the order of magnitude of zonal and tesseral harmonics[15] , only J_2 and J_{22} are considered in the Earth's gravitational potential.

$$U = \frac{g_0 R_0^2}{r}\left(1 - J_2\frac{R_0^2}{r^2}\left(\frac{3\sin^2\phi - 1}{2}\right) + 3J_{22}\frac{R_0^2}{r^2}\cos^2\phi\cos 2\gamma\right) \tag{2}$$

The accelerations caused by Earth's gravitational potential are expressed as[16]

$$\begin{aligned} (a_r)_{ENP} &= \frac{\partial U}{\partial r} = -\frac{g_0 R_0^2}{r^2} - \frac{3J_2 g_0 R_0^4}{2r^4} - \frac{9J_{22} g_0 R_0^4}{r^4}\cos 2\gamma \\ (a_\lambda)_{ENP} &= \frac{1}{r\cos\phi}\frac{\partial U}{\partial \lambda} = -\frac{6J_{22} g_0 R_0^4}{r^4}\sin 2\gamma \end{aligned} . \tag{3}$$

The equations of motion for satellites in the geostationary are obtained by combining Eq. (3) and Eq. (1).

$$\begin{aligned} \ddot{r} - r\left(\Omega + \dot{\lambda}\right)^2 &= -\frac{g_0 R_0^2}{r^2} - \frac{3J_2 g_0 R_0^4}{2r^4} - \frac{9J_{22} g_0 R_0^4}{r^4}\cos 2\gamma \\ r\ddot{\lambda} + 2\dot{r}\left(\Omega + \dot{\lambda}\right) &= -\frac{6J_{22} g_0 R_0^4}{r^4}\sin 2\gamma \end{aligned} \tag{4}$$

A fourth-order equation in λ is obtained by successive differentiation of Eq. (4). Dropping the first and fourth order derivative terms yields[16]

$$\ddot{\lambda} = 18\Omega_E^4 J_{22}\frac{R_0^2}{r^2}\sin 2\left(\lambda - \lambda_{22}\right). \tag{5}$$

In order to exploit the natural dynamics instead of eliminating it, we proceed with the phase-space study of the long-term dynamical model shown in Eq. (5). As depicted in Fig. 1, the solutions of the Eq. (5) are represented as level curves for the one degree of freedom model in the $\left(\lambda, \dot{\lambda}\right)$ plane. It produces two resonance islands centered around two stable equilibrium solutions of Eq. (5) (at $\lambda = 75°$ and $\lambda = 255°$) and two separatrices of the unstable points (at $\lambda = 165°$ and $\lambda = 345°$).

2.2 East-west station-keeping strategy

Low-thrust station-keeping maneuvers in the existed studies are focusing on the eliminations of the natural drift, which is implemented about once per day, resulting in a disorganized controlled motion around the longitude slot center. However, since the phase-space exploration of the geosynchronous resonance reveals an interesting feature, namely any GEO satellite can be related with a coast arc centered at $\left(\lambda = \lambda_i, \dot{\lambda} = 0\right)$, low-thrust maneuvers can also jointly work in cooperation with the natural drift to form the boundary-to-boundary motion in the predefined longitude slot, in analogy of what is already done for chemical propelled GEO satellites.

DOI: 10.13009/EUCASS2019-723

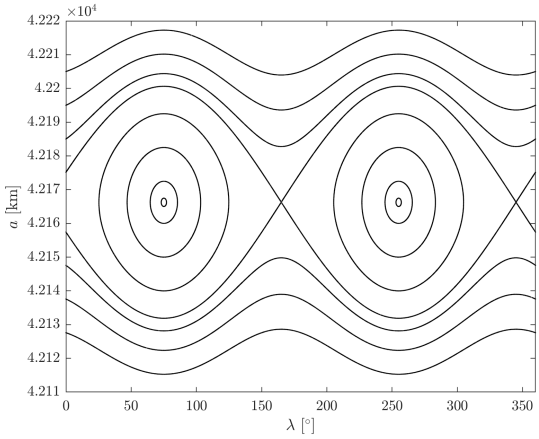

Figure 1: Phase space for a geostationary orbit in resonance with J_{22}.

Minimum-time and minimum-fuel optimizations provide the practical alternatives to achieve the low-thrust boundary-to-boundary motion. Moreover, since minimum-time method works as the preliminary of the minimum-fuel method, this section models and solves two methods in order.

On the contrary to the long-term representation of the coast arcs, osculating dynamics including both zonal and tesseral harmonics are considered in the thrust arcs. Thus, the two-dimensional dynamics of the thrust arcs are written in condense form as

$$\begin{cases} \dot{\mathbf{x}} = \frac{uT}{m}\mathbf{A}(\mathbf{x})\,\mathbf{d} + \mathbf{B}(\mathbf{x}) \\ \dot{m} = -\frac{uT}{I_{sp}g_0} \end{cases} \tag{6}$$

Where $\mathbf{x} = \left(r, \dot{r}, \lambda, \dot{\lambda}\right)^T$ denotes the in-plane variables, $\mathbf{d} = \left(d_r, d_\lambda, d_\phi\right)^T$ denotes the thrust unit vector, $u \in [0, 1]$ is the throttle factor, T is the thrust magnitude, $\mathbf{A}(\mathbf{x})$ and $\mathbf{B}(\mathbf{x})$ are matrices of 4×3, which can be derived from Eq. (1) and Eq. (3).

The objective function of minimum-time (MT) problem[14] is shown in Eq. (7), resulting in the hamitonian written as Eq. (8).

$$J_{MT} = \int_{t_i}^{t_f} 1 dt \tag{7}$$

$$H_{MT} = \mathbf{p_x}^T \cdot \left(\frac{uT}{m}\mathbf{A}(\mathbf{x})\,\mathbf{d} + \mathbf{B}(\mathbf{x})\right) - p_m \cdot \frac{uT}{I_{sp}g_0} + 1 \tag{8}$$

While the objective function of minimum-fuel (MF) problem[13] is shown in Eq. (9), resulting in the Hamiltonian written as Eq. (10).

$$J_{MF} = \frac{T}{I_{sp}g_0}\int_{t_i}^{t_f} (u - \varepsilon u(1-u))\, dt \tag{9}$$

$$H_{MF} = \mathbf{p_x}^T \cdot \left(\frac{uT}{m}\mathbf{A}(\mathbf{x})\,\mathbf{d} + \mathbf{B}(\mathbf{x})\right) - p_m \cdot \frac{uT}{I_{sp}g_0} + \frac{T}{I_{sp}g_0}(u - \varepsilon u(1-u)) \tag{10}$$

where $\varepsilon \to 0$.

Minimum-time and minimum-fuel methods share the procedures to define the variational equations of costates $[\dot{\mathbf{p}}_\mathbf{x}, \dot{p}_m]^T$ and the optimal thrust unit vector $\mathbf{d}^*$, which is illustrated in Eq. (11) and Eq. (12), respectively.

$$\dot{\mathbf{p}} = \begin{bmatrix} \dot{\mathbf{p}}_\mathbf{x} \\ \dot{p}_m \end{bmatrix} = \begin{bmatrix} -\frac{\partial H}{\partial \mathbf{x}} \\ -\frac{\partial H}{\partial m} \end{bmatrix} = \begin{bmatrix} -\mathbf{p_x}^T \cdot \left(\frac{uT}{m}\mathbf{C}(\mathbf{x},\mathbf{d}) + \mathbf{D}(\mathbf{x})\right) \\ \mathbf{p_x}^T \frac{uT}{m^2}\mathbf{A}(\mathbf{x})\,\mathbf{d} \end{bmatrix} \tag{11}$$

Where $\mathbf{C}(\mathbf{x},\mathbf{d})$ and $\mathbf{D}(\mathbf{x})$ are the 4×3 Jacobian matrices of $\mathbf{A}(\mathbf{x})$ and $\mathbf{B}(\mathbf{x})$, $\mathbf{C}(\mathbf{x},\mathbf{d}) = \frac{\partial(\mathbf{A}(\mathbf{x})\mathbf{d})}{\partial \mathbf{x}}$, $\mathbf{D}(\mathbf{x}) = \frac{\partial \mathbf{B}(\mathbf{x})}{\partial \mathbf{x}}$.

$$\mathbf{d}^* = -\frac{\mathbf{A}^T\mathbf{p_x}}{\left\|\mathbf{A}^T\mathbf{p_x}\right\|} \tag{12}$$

DOI: 10.13009/EUCASS2019-723

Thus, differential equations of states and costates for minimum-time and minimum-fuel methods can be written as

$$\begin{aligned}
&\dot{\mathbf{x}} = \frac{uT}{m}\mathbf{A}(\mathbf{x})\,\mathbf{d}^* + \mathbf{B}(\mathbf{x}) \\
&\dot{m} = -\frac{uT}{I_{sp}g_0} \\
&\dot{\mathbf{p}}_\mathbf{x} = -\mathbf{p}_\mathbf{x}{}^T \cdot \left(\frac{uT}{m}\frac{\partial(\mathbf{A}(\mathbf{x})\mathbf{d}^*)}{\partial \mathbf{x}} + \frac{\mathbf{B}(\mathbf{x})}{\partial \mathbf{x}}\right) \\
&\dot{p}_m = -\frac{uT}{m^2}\left\|\mathbf{A}^T\mathbf{p}_\mathbf{x}\right\|
\end{aligned} \tag{13}$$

However, there are two main differences of these two methods. The first is in the derivation of the optimal throttle factor u^* .

Substituting optimal thrust unit vector $\mathbf{d}^*$ into two Hamiltonians leads to

$$H_{MT} = \mathbf{p}_\mathbf{x}{}^T\mathbf{B}(\mathbf{x}) + \frac{uT}{I_{sp}g_0}\left(-\frac{I_{sp}g_0}{m}\left\|\mathbf{A}^T\mathbf{p}_\mathbf{x}\right\| - p_m\right)\cdot +1 \tag{14}$$

$$H_{MF} = \mathbf{p}_\mathbf{x}{}^T \cdot \mathbf{B}(\mathbf{x}) + \frac{uT}{I_{sp}g_0}\left(-\frac{I_{sp}g_0}{m}\left\|\mathbf{A}^T\mathbf{p}_\mathbf{x}\right\| - p_m + 1 - \varepsilon + \varepsilon u\right) \tag{15}$$

Defining switching function S_{MT} and S_{MF} as

$$S_{MT} = -\frac{I_{sp}g_0}{m}\left\|\mathbf{A}^T\mathbf{p}_\mathbf{x}\right\| - p_m \tag{16}$$

$$S_{MF} = -\frac{I_{sp}g_0}{m}\left\|\mathbf{A}^T\mathbf{p}_\mathbf{x}\right\| - p_m + 1 \tag{17}$$

Differentiating the switching functions and using Pontryagin's Maximum Principle yields

$$\begin{cases} {u_{MT}}^* = 0 & if\ S_{MT} > 0 \\ {u_{MT}}^* \in [0,1] & if\ S_{MT} = 0 \\ {u_{MT}}^* = 1 & if\ S_{MT} < 0 \end{cases} \tag{18}$$

$$\begin{cases} {u_{MF}}^* = 0 & if\ S_{MF} > \varepsilon \\ {u_{MF}}^* = \frac{\varepsilon - S}{2\varepsilon} & if\ -\varepsilon \le S_{MF} \le \varepsilon \\ {u_{MF}}^* = 1 & if\ S_{MF} < -\varepsilon \end{cases} \tag{19}$$

On the other hand, since a minimum-time step is first solved to infer the minimum possible transfer time $t_{f_{\min}}$, the constraints of minimum-time problem (Eq. (20)) and minimum-fuel problem (Eq. (21)) are different.

$$\begin{cases} \mathbf{x}(t_i) = \mathbf{x}_i \\ m(t_i) = m_i \\ \mathbf{x}\left(t_f\right) = \mathbf{x}_f \\ p_m\left(t_f\right) = 0 \\ H\left(t_f\right) = 0 \end{cases} \tag{20}$$

$$\begin{cases} \mathbf{x}(t_i) = \mathbf{x}_i \\ m(t_i) = m_i \\ \mathbf{x}\left(t_f\right) = \mathbf{x}_f \\ p_m\left(t_f\right) = 0 \\ t_f \ge t_{f_{\min}} \end{cases} \tag{21}$$

To solve the Two Point Boundary Value Problem (TPBVP) described by Eq. Eq, a three-step method is applied to guess the values of initial costates $\left[\mathbf{p}_\mathbf{x}(t_i), p_m(t_i)\right]^T$ and final time t_f .

(1) An impulsive solution is first calculated and regarded as the center of the thrust arc to formulate the continuous thrust solution;

(2) Based on continuous thrust solution, updating $\left[\mathbf{p}_\mathbf{x}(t_i), p_m(t_i)\right]^T$ and t_f through Matlab function fsolve or fmincon with minimum-time constraints;

(3) Based on minimum-time solution, updating $\left[\mathbf{p}_\mathbf{x}(t_i), p_m(t_i)\right]^T$ and t_f through Matlab function fsolve or fmincon with minimum-fuel constraints.

DOI: 10.13009/EUCASS2019-723

3. Out-of-plane motion and North-south station-keeping

This section extends the two-dimensional equations of motion into a three dimensional controlled dynamics. The effects of the luni-solar perturbations are analyzed to define the latitude (inclination) slot. Minimum-time and minimum-fuel optimized tools are applied to achieve the boundary-to-boundary motion within a given latitude (inclination) slot.

3.1 Three-dimensional controlled dynamics

With the aim of analysis on the out-of-plane motion for GEO satellites, the two-dimensional equations of motion due to the Earth's gravity field is extended into a three-dimensional model, shown as Eq. (22).

$$\begin{aligned}
&\ddot{r} - r\left(\Omega+\dot{\lambda}\right)^2\cos^2\phi - r\dot{\phi}^2 = -\frac{g_0R_0^2}{r^2} + \frac{3J_2g_0R_0^4}{2r^4}\left(3\sin^2\phi - 1\right) - \frac{9J_{22}g_0R_0^4}{r^4}\cos^2\phi\cos 2\gamma \\
&r\cos\phi\ddot{\lambda} + 2\dot{r}\left(\Omega+\dot{\lambda}\right)\cos\phi - 2r\left(\Omega+\dot{\lambda}\right)\dot{\phi}\sin\phi = -\frac{6J_{22}g_0R_0^4}{r^4}\cos\phi\sin 2\gamma \\
&2\dot{r}\dot{\phi} + r\ddot{\phi} + r\left(\Omega+\dot{\lambda}\right)^2\cos\phi\sin\phi = -\frac{3J_2g_0R_0^4}{r^4}\sin\phi\cos\phi - \frac{6J_{22}g_0R_0^4}{r^4}\cos\phi\sin\phi\cos 2\gamma
\end{aligned} \tag{22}$$

Moreover, in order to assess the possibility of station-keeping in latitude slot, lunisolar perturbations, which mainly affect the evolution of inclination, are considered. Then Acceleration components in the Earth-fixed spherical coordinate system due to luni-solar perturbations are written as[16]

$$\begin{aligned}
(a_r)_{LSP} &= r\dot{\alpha}^2\left(3\left(a_x\cos\alpha + a_y\sin\alpha\right)^2 - 1\right) + \frac{r\dot{\nu}^2}{\mu}\left(3\left(a_x\cos\nu + a_y\sin\nu\right)^2 - 1\right) \\
(a_\lambda)_{LSP} &= 3r\dot{\alpha}^2\left(a_x\cos\alpha + a_y\sin\alpha\right)\left(b_x\cos\alpha + b_y\sin\alpha\right) + \frac{3r\dot{\nu}^2}{\mu}\left(a_x\cos\nu + a_y\sin\nu\right)\left(b_x\cos\nu + b_y\sin\nu\right) \\
\left(a_\phi\right)_{LSP} &= 3r\dot{\alpha}^2\left(a_x\cos\alpha + a_y\sin\alpha\right)\left(c_x\cos\alpha + c_y\sin\alpha\right) + \frac{3r\dot{\nu}^2}{\mu}\left(a_x\cos\nu + a_y\sin\nu\right)\left(c_x\cos\nu + c_y\sin\nu\right)
\end{aligned} \tag{23}$$

Where earth-moon system center moves around the sun with a constant angular rate $\dot{\alpha}$, and earth-moon system rotates its center with a constant angular rate $\dot{\nu}$, $\left(a_x, a_y, a_z, b_x, b_y, b_z, c_x, c_y, c_z\right)$ are coefficients determined by $(\lambda, \phi, \lambda_{ec})$, λ_{ec} is the angle between the Earth's equatorial plane and ecliptic plane.

3.2 North-south station-keeping

Combing Eq. (23) and Eq. (22) yields the three-dimensional controlled dynamics. According to the numerical integrations based on the three-dimensional controlled dynamics, which is also analytically studied by Wytrzyszczak[17] , by carefully selecting the right ascension of the initial orbital plane along with an inclination of a few degrees, luni-solar perturbations will naturally reduce the inclination to zero before increasing again (see Fig. 2). According to the predefined parameters, the control cycle of north-south station-keeping for GEO satellites can vary from months to years, which determines the latitude (inclination) slot.

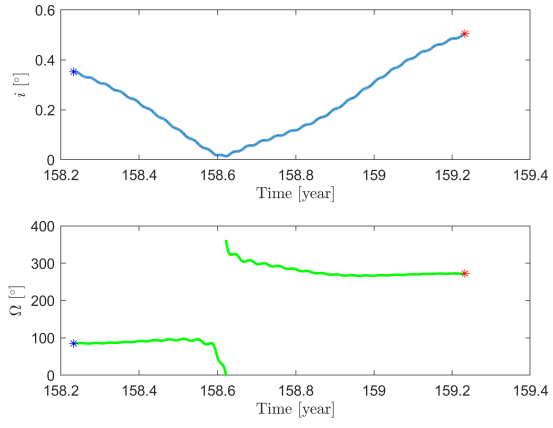

Figure 2: Natural drifts of the inclination and RAAN of a satellite with specified initial state.

In fact, all Soviet GEO spacecraft launched from 1974 through 1993 (more than 100 in all) performed no North-South station-keeping at all[17] . Furthermore, according to the report "Classification of Geosynchronous Objects"[18] ,

DOI: 10.13009/EUCASS2019-723

which is published by European Space Agency (ESA) in 2018, over 100 on-orbit GEO satellites are currently working without North-South Station-keeping, which definitely increases the lifetime.

Therefore, the north-south station-keeping strategy proposed in this work is to employ luni-solar perturbation and low-thrust maneuvers to accomplish the boundary-to-boundary motion in such predefined latitude (inclination) slot, which can be better understood though the three phase-space plots in scenario c of simulations and results.

As for the design of the low-thrust maneuver, minimum-time and minimum-fuel optimization tools are used with similar procedures as the proposed methods in section implemented. To note, with out-of-plane motion required, state variables $\mathbf{x} = \left[r, \dot{r}, \lambda, \dot{\lambda}, \phi, \dot{\phi}, m\right]^T$ and costates $\mathbf{p_x} = \left[p_r, p_{\dot{r}}, p_\lambda, p_{\dot{\lambda}}, p_\phi, p_{\dot{\phi}}, p_m\right]^T$ are reconstructed as well as matrices $\mathbf{A}(\mathbf{x}), \mathbf{B}(\mathbf{x}), \mathbf{C}(\mathbf{x}, \mathbf{d}), \mathbf{D}(\mathbf{x})$.

4. Simulations and results

East-west station-keeping and north-south station-keeping strategies are separately validated in this section. All the satellites in this section share the initial mass $m_0 = 2000kg$ and are equipped with the same electric propulsion system $T = 200mN$.

Scenario A is to conduct comparisons between the minimum-time and minimum-fuel methods of east-west station-keeping, which in concluded in Table 1. Since we design the throttle factor u in the optimization model, the duration of thrust arc displayed in Table 1 is accumulated only if the thruster is on. All the satellites are centered at $\lambda = 60°$, while slot width varies. Using minimum-fuel method, the fuel consumption of the satellite located at $[60°, 60° + 0.1°]$ decreases by $[60°, 60° + 0.1°]$ with respect to that of minimum-time method. This ratio is increasing with the increase of the slot width. From sustainable point of view, increasingly crowded GEO region results in more limited slots and requires more accurate station-keeping, which further increase the operational costs. Thus, both highly efficient station-keeping strategy and end-of-life disposal should be of great concern.

Table 1: Comparisons between minimum-time and minimum-fuel methods in East-west sation-keeing

	Slot Center [°]	Slot width [°]	Control cycles	DCA[a] [$days$]	DTC[b] [s]	VB[b] [m/s]
Minimum-time	60	0.5	5	346.4	31594	3.1595
Minimum-fuel	60	0.5	5	345.7	31570	3.1568
Minimum-time	60	0.1	11	341.07	48843	4.884
Minimum-fuel	60	0.1	11	350.61	48812	4.881
Minimum-time	60	0.01	35	341.9	89649	8.649
Minimum-fuel	60	0.01	35	342	89537	8.9537

[a]Duration of coast arc, [b]Duration of thrust arc, [c]Velocity budget

Since typically predefined geostationary slot is usually defined as a volume centered on a specific longitude with a size of 0.1°, scenario B applies our east-west station-keeping strategy to 360 slots from 0 to 2π with slot width equal 0.1° . The left column of Fig. 3 shows the station-keeping cycles, consisting of one coast arc and one thrust arc, centered at the longitudes ranging from 73° to 77° . For the satellite centered at the stable equilibria $\lambda = 75°$, the duration of the coast arc is much longer than that in the neighborhood slots, which can be further explained through the Fig. 4 and Fig. 5.

As shown in the right column of Fig. 3, taking the GEO satellite located at 70° as an example, the designed low-thrust arc is convex with respect to the impulsive arc, which is a straight line because of the instantaneous maneuver. Another thing worthy mention is that boundary-to-boundary motion in the longitude slot allows for a convenient GEO satellite collocation, which offers an approach to maximise the use of the GEO resources. Namely, collocated satellites are distributed in different phases during their natural drifting part, such that no further control rather than a pre-set phase is required for their collocation within the slot.

Further investigations about the characteristics of equatorial station-keeping are implemented and the results are shown in Fig. 4 and Fig. 5. The durations of one cycle of satellites in different slots are distributed in the wave-like curve as well as the associated velocity budgets of station-keeping (see Fig. 4). Stable and unstable solutions in the longitude phase space represent the slots of best performances, where the single station-keeping cycle lasts long and velocity increment remains low. Moreover, the long-durational performance of the proposed method the is further identified by computing the time and fuel maps though the data of 10 station-keeping cycles, shown in Fig. 5.

Scenario C is used to validate North-south station-keeping strategy. Note that, the performance of the proposed NSSK can be clearly analyzed through combining three different plots, namely the inclination phase space $(i \sin\Omega, i \cos\Omega)$, the latitude phase space $\left(\phi, \dot{\phi}\right)$ and the time histories of inclination and right ascension of the ascending node (RAAN). Time histories of the inclination and RAAN (left column of Fig. 6) directly point out that the

DOI: 10.13009/EUCASS2019-723

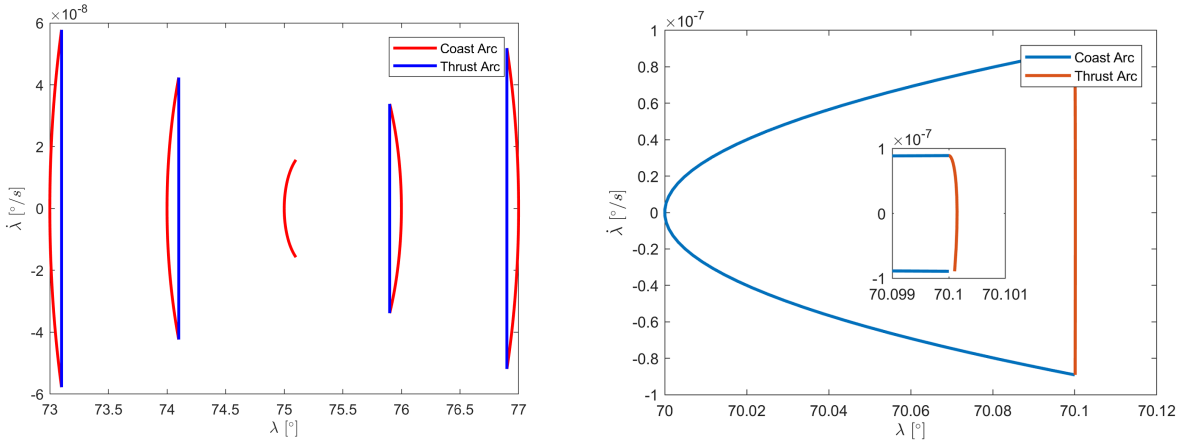

Figure 3: Boundary-to-boundary motion within a longitude slot. The left column corresponds to 5 slots centered at longitudes ranging from 73° to 77° and the right column to the single slot centered at $\lambda = 70°$.

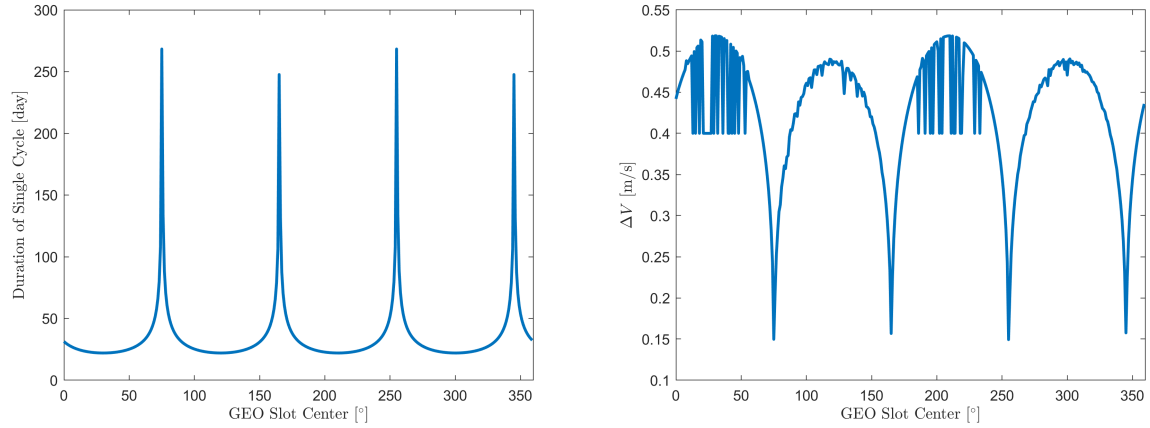

Figure 4: Distribution of the averaging duration of single station-keeping cycle (left column) and averaging velocity budget (right column) in different longitude slots.

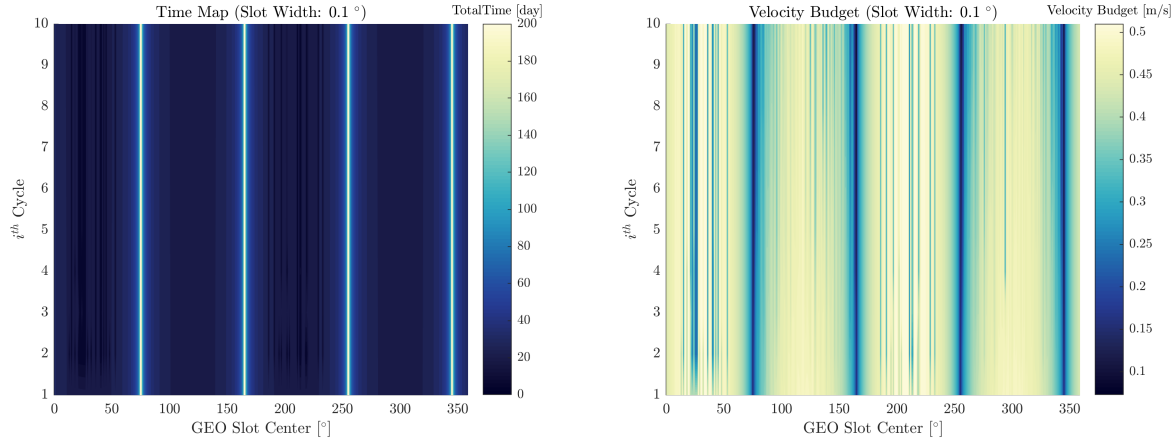

Figure 5: Time (left column) and velocity budget (right column) maps computed by simluations of 360 slots and 10 control cycles.

key of north-south station-keeping is to repeat boundary-to-boundary motion within the preset inclination by changing RAAN. Red and purple curves in the inclination phase space , displayed in the right column of Fig. 6, represent the

DOI: 10.13009/EUCASS2019-723

low-thrust maneuvers, which contains a thrust direction reversion when the satellite passes by ascending or descending node. The latitude phase space $(\phi, \dot{\phi})$ and the time history of latitude, shown in Fig. 7, can be characterized as the front view and left view of a "three-dimensional latitude pipe", which owns the spiral circulation with "convergency - divergency" tendency.

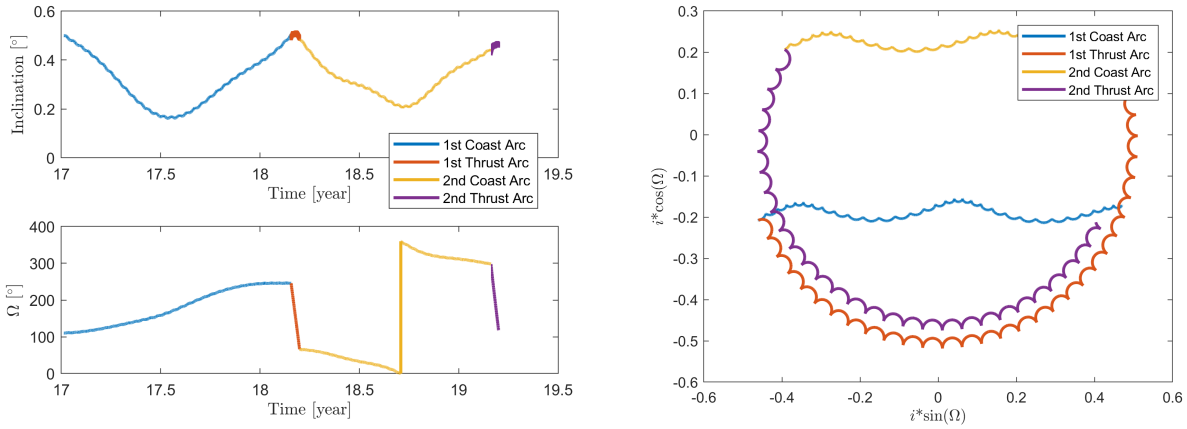

Figure 6: Time histories of the inclination and RAAN (left column) and inclination phase space corresponding to the boundary-to-boundary motion in a inclination slot.

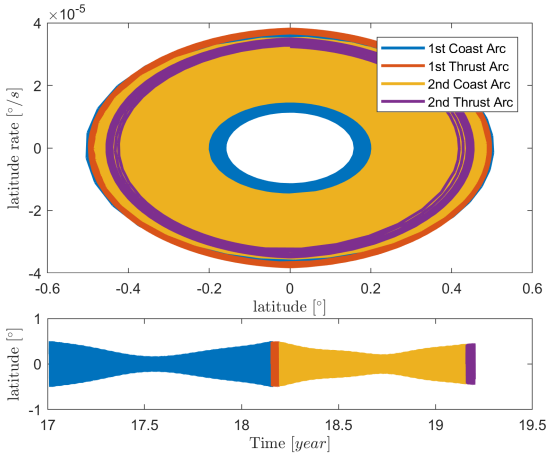

Figure 7: Latitude phase space (upper row) and time history of latitude (bottom row) corresponding to the boundary-to-boundary motion in a inclination slot.

The effects of the increase in initial inclination on the bounded motion within a latitude slot are discussed in Table 2, which provides an alternative to perform with none or few north-south station-keeping. Compared to east-west station-keeping, with the aim of stay in a slot with equal slot width, the velocity budget of north-south station-keeping is one order of magnitude higher, proving the great potential in cost saving by exploiting natural dynamics, especially in latitude direction.

Table 2: Comparions of the north-south station-keeping method for satellites with different inital inclination

	Duration of Coast Arc	Duration of Thrust Arc	Velocity Budget
Case 1: $i_0 = 0.5°$	417.40 days	15.60 days	135 m/s
Case 2: $i_0 = 0.35°$	256.95 days	10.54 days	91.54 m/s
Case 3: $i_0 = 0.1°$	78.35 days	2.88 days	24.88 m/s

DOI: 10.13009/EUCASS2019-723

5. Conclusion

In this work, we have investigated the problem of low-thrust geostationary station-keeping. Dynamical model due to Earth's triaxiality and luni-solar attraction is revisited based on the spherical coordinate representation. We have studied the reduced longitude phase-space by computing the equilibrium points and inclination phase-space through numerical integration on the out-of-plane motion of equation. According to the phase-space studies, the boundary-to-boundary motions within a given longitude slot and an inclination slot are designed to combine low-thrust maneuvers jointly with the exploitation of the natural dynamics. Minimum-time and minimum-fuel methods are used to design the low-thrust maneuvers, while initial costates evaluation method is proposed to solve the two point boundary value problem. East-west station-keeping strategy is applied to the whole GEO region and achieve good long-term performance. Since inclination slot with specified initial inclination and RAAN.

As further work, we will analytically compute the equilibria in the latitude phase space. Moreover, additional perturbation terms can be added in our model to make the approximation more accurate. This will help us to evaluate the performance of station-keeping strategy with orbits in the full model and allow us to check if they hold the desired properties. Analytical formulation of the initial costates and final time can be developed based on the appropriate assumption concluded from the phase-space study, which can improve the computational efficiency of two point boundary value problem.

6. Acknowledgments

This project has received funding from the European Research Council (ERC) under the European Union's Horizon 2020 research and innovation programme (grant agreement No.679086-COMPASS) and the National Natural Science Foundation of China (No. 11772051).

References

[1] C. Christian, U. Carlo O. Emiliano, , and A. Tommaso. Possible alternative to geostationary earth orbit. *Journal of Guidance, Control and Dynamics*, 38(3):534–539, 2015.

[2] C. Colombo. Planetary orbital dynamics (planodyn) suite for long term propagation in perturbed environment. 6th International Conference on As- trodynamics Tools and Techniques, 2016.

[3] I. Gkolias, M. Lara, and C. Colombo. An ecliptic perspective for analytical satellite theories. AIAA/AAS Astrodynamics Specialist Conference, 2018.

[4] T. A. Ely. Dynamics and control of artificial satellite orbits with multiple tesseral resonances. PhD Thesis, Purdue University, 1996.

[5] N. L. Johnson. A new look at the geo and near-geo regimes: Operations, disposals,anddebris. *Acta Astronautica*, 80:82–88, 2012.

[6] I. Gkolias and C. Colombo. Towards a sustainable exploitation of the geosynchronous orbital region. *Celestial Mechanics and Dynamical Astronomy*, 131:1–30, April 2019.

[7] C. Colombo. Long-term evolution of highly-elliptical orbits: luni-solar perturbation effects for stability and re-entry. *Frontiers in Astronomy and Space Science*, pages 1–31, April 2019.

[8] F. J. de Bruijn, S. Theil, and E. Gill D. Choukroun. Geostationary satellite station-keeping using convex optimization. *Journal of Guidance, Control and Dynamics*, 39(3):605–616, March 2016.

[9] F. J. de Bruijn, S. Theil, D. Choukroun, and E. Gill. Collocation of geostationary satellites using convex optimization. *Journal of Guidance, Control and Dynamics*, 39(6):1303–1313, 2016.

[10] D. Losa. High vs low thrust station keeping maneuver planning for geostationary satellites. PhD Thesis, Ecole Nationale Superieure des Mines de Paris, 2007.

[11] C. Gazzino, D. Arzelier, C. Louembet, C. Cerri, C. Pittet, and D. Losa. Long-term electric-propulsion geostationary station-keeping via integer programming. *Journal of Guidance, Control and Dynamics*, 42(5):976–991, May 2019.

DOI: 10.13009/EUCASS2019-723

[12] L. Li, J. Zhang, S. Zhao, and A. Shi. Autonomous station-keeping strategy for geostationary satellite with electric propulsion system. 68th International Astronautical Congress, 2017.

[13] C. Zhang, F. Topputo, F. B. Zazzera, and Y. Zhao. Low-thrust minimum-fuel optimization in the circular restricted three-body problem. *Journal of Guidance, Control and Dynamics*, 38(8):1501–1509, August 2015.

[14] S. Zhao, P. Gurfil, and J. Zhang. Initial costates for low-thrust minimum-time station change of geostationary satellites. *Journal of Guidance, Control and Dynamics*, 39(12), December 2016.

[15] H. Li. Geostationary satellite orbital analysis and collocation strategies. National Defense Industry Press, 2010.

[16] R. H. Frick and T. B. Garber. Perturbations of a synchronous satellites. Technical report, National aeronautics and space administration, May 1962.

[17] I. Wytrzyszczak. Testing the safety of decommissioned spacecraft above geo. *Advances in Space Research*, 34:1209–1213, 2004.

[18] S. Lemmens. Classification of geosynchronous objects: Produced with the discos database. Technical report, ESA's Space Debris Office, May 2018.